



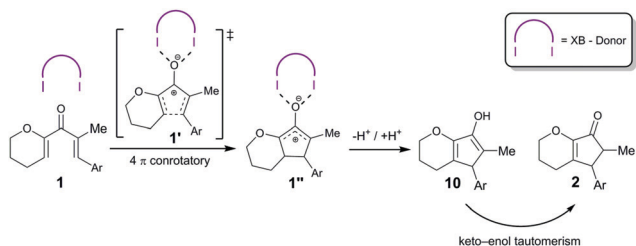
after a few weeks for the neutral multidentate polyfluorinated XB donors **3**, **4** and **5**, as well as for the monodentate cationic XB donor **6**. The inactivity of the former class of compounds, which are all active in halide abstraction reactions,<sup>10</sup> illustrates the additional challenges associated with the activation of neutral substrates like divinyl ketones. As the reaction seemed to require stronger Lewis acids as catalysts, bidentate cationic XB donors were studied next. These were successfully used in a Diels–Alder and a Michael addition reaction,<sup>14,15</sup> and in both cases a strong influence of the counterion was observed: satisfactory performance could only be achieved with noncoordinating anions like tetrakis[3,5-bis(trifluoromethyl)-phenyl]borate (**BARF<sub>4</sub>**) but not with counterions like triflate. Somewhat surprisingly, however, the triflate as well as the **BARF<sub>4</sub>** salt of bis(imidazolium) derivative **7** showed no catalytic activity in this reaction – despite their earlier mentioned success in carbonyl activation reactions. Apparently, the Lewis acidity of these compounds is too low to allow sufficient reduction of the activation barrier, and thus the more electrophilic bis(benzimidazolium) derivatives **8** and **9** were investigated. The triflate salt of the direct benzimidazolium analogue, **8/OTf**, leads to hardly noticeable formation of product **2** ( $\leq 5\%$ ) after 5 hours (Table 1).<sup>17</sup>

The corresponding **BARF<sub>4</sub>** salt, on the other hand, showed a markedly increased performance (full consumption of **1** after 2 h with 5 mol% catalyst), which is in line with the noncoordinating nature of this counterion. In the <sup>1</sup>H-NMR spectra of the reaction, next to the chemical shifts of starting material **1** and product **2**, an additional set of signals was observed over time, which likely correspond to enol **10** (see Scheme 2 and the ESI†). An example for such spectra (with compound **syn-9/OTf** as a catalyst) is depicted in Fig. 1.

Table 1 Performance of catalyst candidates

Cat. (mol%)	Yield of <b>10</b> (5 h)	Yield of <b>2</b> (5 h) <sup>a</sup>	<i>cis/trans</i> ratio of <b>2</b> <sup>d</sup>
None	—	—	—
<b>3–7</b> (5)	—	$\leq 5\%$	—
<b>8/OTf</b> (5)	$< 5\%$	$\leq 5\%$	—
<b>8/BARF<sub>4</sub></b> (5)	71%	26%	3 : 1
<b>syn-9/OTf</b> (5)	70%	23%	2.3 : 1
<b>syn-9/BARF<sub>4</sub></b> (5)	20%	65%	2 : 1
<b>11–13</b> (5)	—	—	—
HOTf (1)	—	$\geq 95\%$	6.5 : 1
I <sub>2</sub> (5)	—	$\geq 95\%$ <sup>b</sup>	2.3 : 1 <sup>b</sup>
<b>syn-9/OTf</b> (5) <sup>c</sup>	6% <sup>c</sup>	90% <sup>c</sup> (80%) <sup>d</sup>	2.3 : 1

$c_0(\mathbf{1}) = 15.4$  mM in CD<sub>2</sub>Cl<sub>2</sub>. <sup>a</sup> Determined by <sup>1</sup>H NMR. <sup>b</sup> After 1 h. <sup>c</sup>  $c_0(\mathbf{1}) = 655.4$  mM in CD<sub>2</sub>Cl<sub>2</sub> and reaction time 12 h. <sup>d</sup> Isolated yields.



Scheme 2 Postulated mechanism of the halogen bond catalysed Nazarov reaction.

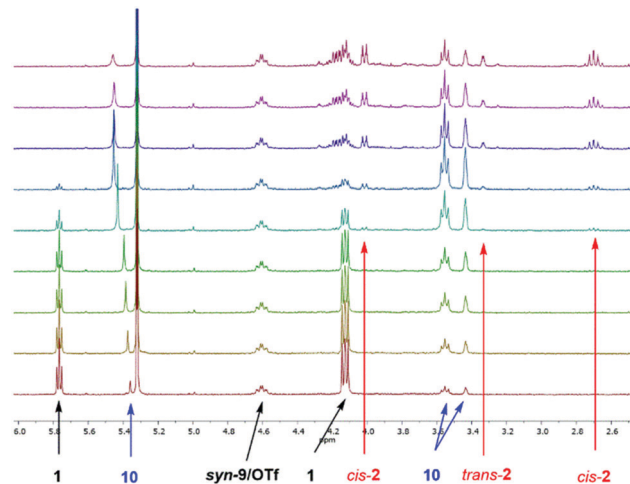


Fig. 1 Selected section of the <sup>1</sup>H-NMR kinetics in CD<sub>2</sub>Cl<sub>2</sub> of the Nazarov reaction ( $c_0(\mathbf{1}) = 15.4$  mM) catalysed by XB Donor **syn-9/OTf** (10 mol%). The <sup>1</sup>H-NMR signals of the corresponding compounds **1**, **2**, **syn-9/OTf** and enol **10** are marked with arrows.

Since we postulate that halogen bonding will only influence the initial step (electrocyclization) of the overall reaction, but not the following keto–enol tautomerization (see Scheme 2), the analysis will first focus on the rate acceleration of the electrocyclization (which can be conveniently monitored *via* the consumption of starting material **1**). The kinetic profile of this step in the presence of catalysts **8** or **9** is shown in Fig. 2.

It becomes immediately apparent that the better performance of **8/BARF<sub>4</sub>** vs. **8/OTf** in overall product formation is also observed in the electrocyclization step. The Lewis acidity of these bidentate XB donors can be further increased by the introduction of a trifluoromethyl group in the central benzene core,<sup>11</sup> which prevents rotation of the XB-donating moieties and allows the isolation of preorganized *syn*-atropisomer **9**. The superior performance of **9** vs. **7** in a halide abstraction case<sup>11</sup> and a Michael addition reaction has been demonstrated before.<sup>14</sup>

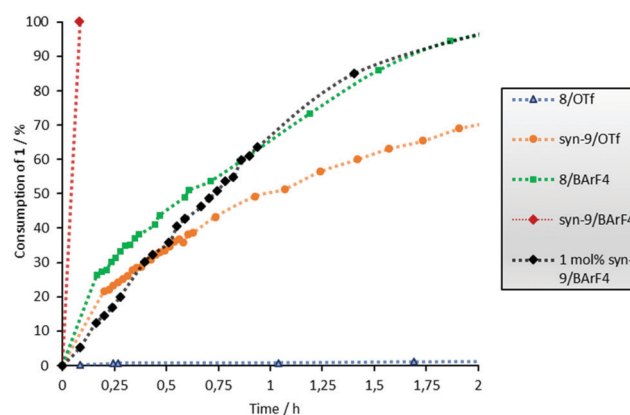


Fig. 2 Consumption of **1** versus the time profile of the Nazarov cyclisation with 5 mol% catalyst (unless noted otherwise) and  $c_0(\mathbf{1}) = 15.4$  mM. No reaction without a catalyst and with compounds **3–7** and **11–13**. The error is approximately 5%.



A strong effect of this preorganization was also found in the Nazarov reaction: triflate salt **syn-9/OTf** showed a markedly better performance compared to its almost inactive analogue **8/OTf** (70% vs. 2% consumption of **1** after 2 h, see Fig. 2). As expected, the highest catalytic activity was achieved with the  $\text{BARF}_4$  salt **syn-9/BARF<sub>4</sub>** – in less than 5 min, and the complete conversion of starting material **1** to enol **10** was observed with only 5 mol% of the catalyst. A reasonable kinetic profile of the electrocyclization step could only be obtained after reducing the amount of catalyst to 1 mol% (Fig. 2). In all cases mentioned so far, the *cis/trans* ratio of product **2** was in the range between 2:1 and 3:1 (Table 1).

Thus, the two key parameters to increase the performance of **8/OTf** are the change of the counterion to  $\text{BARF}_4$  and the introduction of preorganization. Closer inspection of Fig. 2 indicates that the former has a larger impact: exchanging the counterion provides a more active catalyst (**8/BARF<sub>4</sub>**, green line) compared to the more preorganized one with the same counterion (**syn-9/OTf**, orange line).

In order to establish whether the observed activity was in indeed due to halogen bonding, non-iodinated compounds **11**, **12** and **13** were also tested as catalysts (Fig. 3). Even though they share all structural features except the iodine substituents with catalysts **7–9**, none of them showed any activity. Consequently, activation by hydrogen bonding or electrostatic interactions can be ruled out.

Two possible catalytically active decomposition products of the XB donors are elemental iodine and acid traces. A comparison experiment with 5 mol% of elemental iodine showed that it indeed induces quantitative product formation after 30 minutes.<sup>18</sup> The exact origin of this activity is not entirely clear, as elemental iodine has several pathways (XB, hidden acid catalysis<sup>19</sup> or iodonium formation) to activate organic molecules.<sup>20</sup> It is, however, very unlikely that the observed activity of XB donors **8** and **syn-9** is due to the decomposition to elemental iodine, for various reasons: (a) no spectroscopic evidence of decomposition was obtained (only one <sup>19</sup>F signal was observed in the case of **syn-9** after the reaction); (b) the consumption of the starting material follows sigmoidal kinetics with 0.1 mol% of iodine (see Fig. S8 in the ESI† and compare Fig. 2 for **8** and **9**); and (c) a drastically different *cis/trans* ratio of product **2** (23:1) was found with elemental iodine.

Likewise, addition of 1 mol-% of HOTf triggered full conversion of compound **1** to product **2** within 1 hour. The kinetic profile of the acid-catalysed reaction, however, is entirely different from the ones observed for catalysts **8** and **syn-9**, in



Fig. 3 Structures of reference compounds.

which the enol is accumulated (see the ESI†). In addition, the *cis/trans* ratio of product **2** is once again markedly different (6.5:1). As a consequence, catalysis by elemental iodine or acid traces – either as impurities or decomposition products – appears very unlikely and the mode of activation is most probably halogen bonding.

Even though the focus of this study was on the electrocyclization step, it is noteworthy that the rate of the keto–enol tautomerization was apparently not significantly influenced by the catalysts. Also, in some cases the rate of formation of cyclopentenone **2** decreases significantly after full consumption of starting material **1** (see Fig. 4).

Finally, the nature of XB catalysis in this reaction was also investigated by DFT calculations using the M06-2X functional,<sup>21</sup> Grimme D3 dispersion corrections<sup>22</sup> and the def2-TZVP(D) basis set.<sup>23</sup> The corresponding transition state of the Nazarov cyclisation of substrate **1** with a truncated version<sup>24</sup> of XB donor **syn-9** is shown in Fig. 5.

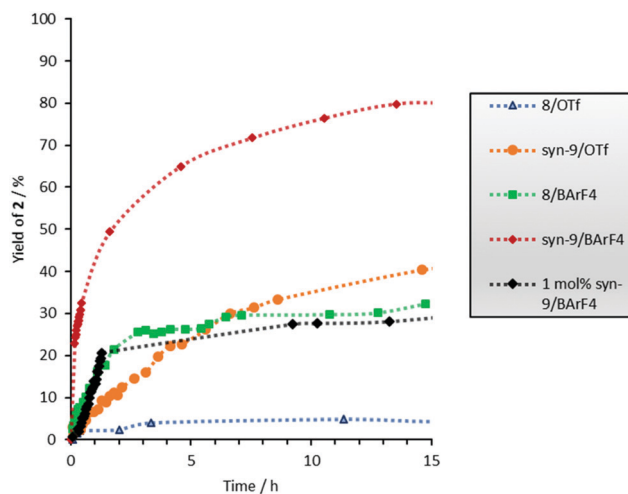


Fig. 4 <sup>1</sup>H-NMR yield vs. time profile for the formation of cyclopentenone **2**. The error is approximately 5%.  $c_0(\mathbf{1}) = 15.4 \text{ mM}$ .

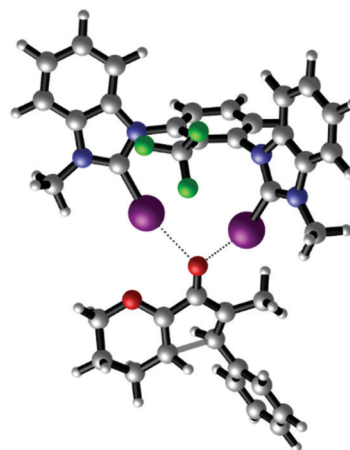


Fig. 5 DFT-calculated transition state structure of the Nazarov cyclisation catalysed by halogen bond-donor **syn-9** (M06-2X D3 def2-TZVP(D)).<sup>25</sup> Selected distances [Å] and angles [°]: I–O 2.68 and 2.69; C–I–O 162 and 164. Graphic generated using CYLview.<sup>26</sup>



The optimized geometry features a clear bidentate binding to the carbonyl oxygen with iodine–oxygen bond distances of 2.68 Å and 2.69 Å. The corresponding barrier of activation (corrected with the SMD18<sup>25</sup> intrinsic solvent model for dichloromethane) is 26.4 kcal mol<sup>-1</sup>. This result is in good agreement with the experimental findings. The barrier for the uncatalysed Nazarov cyclisation (33.1 kcal mol<sup>-1</sup>) is significantly higher.

In conclusion, the first halogen-bonding-catalysed Nazarov cyclisation reaction was reported, which is also just the 4th example of carbonyl activation by this interaction. The catalytic activity could be clearly traced back to halogen bonding *via* comparison experiments. The effect of counterion exchange and preorganization was investigated and compared, and strong performance could only be achieved by a combination of both. In fact, it seems that this reaction is the most challenging one activated by halogen bonding so far (as 7/**BAR**<sup>F</sup><sub>4</sub> did not show any effect in contrast to all examples reported earlier).

This project has received funding from the European Research Council (ERC) under the European Union's Horizon 2020 Research and Innovation Programme (Grant Agreement No. 638337) and from the Fonds der Chemischen Industrie (Dozentenstipendium to S. M. H.). We thank Martin Gartmann for assistance with NMR spectroscopic measurements.

## Conflicts of interest

There are no conflicts to declare.

## Notes and references

- (a) I. N. Nazarov, I. B. Torgov and L. N. Terekhova, *Izv. Akad. Nauk SSSR Otd. Khim. Nauk*, 1942, 200; For the most recent reviews, see: (b) A. J. Frontier and C. Collison, *Tetrahedron*, 2005, **61**, 7577; (c) M. A. Tius, *Eur. J. Org. Chem.*, 2005, 2193; (d) T. Vaidya, R. Eisenberg and A. J. Frontier, *ChemCatChem*, 2011, **3**, 1531; (e) D. R. Wenz and J. Read de Alaniz, *Eur. J. Org. Chem.*, 2015, 23; (f) M. G. Vinogradov, O. V. Turova and S. G. Zlotin, *Org. Biomol. Chem.*, 2017, **15**, 8245.
- (a) G. Liang, S. N. Gradl and D. Trauner, *Org. Lett.*, 2003, **26**, 4931; (b) V. K. Aggarwal and A. J. Belfield, *Org. Lett.*, 2003, **26**, 5075; (c) W. He, X. Sun and A. J. Frontier, *J. Am. Chem. Soc.*, 2003, **125**, 14278; (d) G. Liang and D. Trauner, *J. Am. Chem. Soc.*, 2004, **126**, 9544; (e) K. Murugan, S. Srimurugan and C. Chen, *Chem. Commun.*, 2010, **46**, 1127; (f) G. E. Hutson, Y. E. Türkmen and V. H. Rawal, *J. Am. Chem. Soc.*, 2013, **135**, 4988; (g) J. Davies and D. Leonori, *Chem. Commun.*, 2014, **50**, 15171; (h) T. Mietke, T. Cruchter, V. A. Larionov, T. Faber, K. Harms and E. Meggers, *Adv. Synth. Catal.*, 2018, **360**, 2093.
- (a) M. Vogler, L. Süsse, J. H. W. LaFortune, D. W. Stephan and M. Oestreich, *Organometallics*, 2018, **37**, 3303; (b) L. Süsse, M. Vogler, M. Mewald, B. Kemper, E. Irran and M. Oestreich, *Angew. Chem., Int. Ed.*, 2018, **57**, 11441.
- G. Pouss, A. Devineau, V. Dalla, L. Humphreys, M. Lasne, J. Rouden and J. Blanchet, *Tetrahedron*, 2009, **65**, 10617.
- (a) M. Rueping, W. Ieawsuwan, A. P. Antonchick and B. J. Nachtsheim, *Angew. Chem., Int. Ed.*, 2007, **46**, 2097; (b) A. Jolit, P. M. Walleiser, G. P. A. Yap and M. A. Tius, *Angew. Chem., Int. Ed.*, 2014, **53**, 6180.
- (a) A. K. Basak, N. Shimada, W. F. Bow, D. A. Vivic and M. A. Tius, *J. Am. Chem. Soc.*, 2010, **132**, 8266; (b) A. H. Asari, Y. Lam, M. A. Tius and K. N. Houk, *J. Am. Chem. Soc.*, 2015, **137**, 13199.
- G. R. Desiraju, P. S. Ho, L. Kloo, A. C. Legon, R. Marquardt, P. Metrangolo, P. Politzer, G. Resnati and K. Rissanen, *Pure Appl. Chem.*, 2013, **85**, 1711.
- For the most recent reviews, see: (a) L. C. Gilday, S. W. Robinson, T. A. Barendt, M. J. Langton, B. R. Mullaney and P. D. Beer, *Chem. Rev.*, 2015, **115**, 7118; (b) G. Cavallo, P. Metrangolo, R. Milani, T. Pilati, A. Priimagi, G. Resnati and G. Terraneo, *Chem. Rev.*, 2016, **116**, 2478; (c) D. Bulfield and S. M. Huber, *Chem. - Eur. J.*, 2016, **22**, 14434; (d) R. Tepper and U. S. Schubert, *Angew. Chem., Int. Ed.*, 2018, **57**, 6004.
- (a) S. M. Walter, F. Kniep, E. Herdtweck and S. M. Huber, *Angew. Chem., Int. Ed.*, 2011, **50**, 7187; (b) F. Kniep, L. Rout, S. M. Walter, H. K. V. Bensch, S. H. Jungbauer, E. Herdtweck and S. M. Huber, *Chem. Commun.*, 2012, **48**, 9299; (c) A. Dreger, E. Engelage, B. Mallick, P. D. Beer and S. M. Huber, *Chem. Commun.*, 2018, **54**, 4013.
- F. Kniep, S. H. Jungbauer, Q. Zhang, S. M. Walter, S. Schindler, I. Schnapperle, E. Herdtweck and S. M. Huber, *Angew. Chem., Int. Ed.*, 2013, **52**, 7028.
- S. H. Jungbauer and S. M. Huber, *J. Am. Chem. Soc.*, 2015, **137**, 12110.
- (a) A. Bruckmann, M. A. Pena and C. Bolm, *Synlett*, 2008, 900; (b) W. He, Y. Ge and C. Tan, *Org. Lett.*, 2014, **16**, 3244; (c) K. Matsuzaki, H. Uno, E. Tokunaga and N. Shibata, *ACS Catal.*, 2018, **8**, 6601.
- (a) D. von der Heiden, S. Bozkus, M. Klusmann and M. Breugst, *J. Org. Chem.*, 2017, **82**, 4037; (b) D. von der Heiden, E. Detmar, R. Kuchta and M. Breugst, *Synlett*, 2018, 1307.
- J. Gliese, S. H. Jungbauer and S. M. Huber, *Chem. Commun.*, 2017, **53**, 12052.
- S. H. Jungbauer, S. M. Walter, S. Schindler, L. Rout, F. Kniep and S. M. Huber, *Chem. Commun.*, 2014, **50**, 6281.
- (a) Y. Takeda, D. Hisakuni, C. Lin and S. Minakata, *Org. Lett.*, 2015, **17**, 318; (b) R. Haraguchi, S. Hoshino, M. Sakai, S. Tanazawa, Y. Morita, T. Komatsu and S. Fukuzawa, *Chem. Commun.*, 2018, **54**, 10320; (c) F. Heinen, E. Engelage, A. Dreger, R. Weiss and S. M. Huber, *Angew. Chem., Int. Ed.*, 2018, **57**, 3892.
- After longer reaction times, formation of product 2 is observed with sigmoidal kinetics (Fig. S4, ESI<sup>†</sup>). Currently, we cannot explain their origin.
- Lower amounts of iodine lead to sigmoidal kinetics, see Fig. S8 in the ESI<sup>†</sup>.
- T. T. Dang, F. Boeck and L. Hintermann, *J. Org. Chem.*, 2011, **76**, 9353.
- M. Breugst and D. von der Heiden, *Chem. - Eur. J.*, 2018, **24**, 9187.
- Y. Zhao and D. G. Truhlar, *Theor. Chem. Acc.*, 2008, **120**, 215.
- S. Grimme, J. Antony, S. Ehrlich and H. Krieg, *J. Chem. Phys.*, 2010, **132**, 154104.
- This basis set consists of def2-TZVP (F. Weigend, R. Ahlrichs, *Phys. Chem. Chem. Phys.*, 2005, **7**, 3297) for all main group elements up to Kr and def2-TZVPD (D. Rappoport, F. Furche, *J. Chem. Phys.* 2010, **133**, 134105) for all other elements.
- The counterion (**BAR**<sup>F</sup><sub>4</sub>) and the *para*-fluorine substituent of the aryl group of the substrate were omitted and the *N*-octyl-chains were exchanged to *N*-methyl for reasons of computational costs.
- E. Engelage, N. Schulz, F. Heinen, S. M. Huber, D. G. Truhlar and C. J. Cramer, *Chem. - Eur. J.*, 2018, **24**, 15983.
- Legault, C. Y. CYLview, 1.0b; Université de Sherbrooke: Sherbrooke, 2009, <http://www.cylview.org>.

